RP Materials: Proceedings
Vol. 1, Part 1 (2022) pp. 22–25
e-ISSN:

RESEARCH PLATEAU PUBLISHERS

Cite this article: V. Chahal, Performance evaluation of integrated-optic microring resonators for sensing applications, *RP Materials: Proceedings* Vol. 1, Part 1 (2022) pp. 22–25.

Original Research Article

Performance evaluation of integrated-optic microring resonators for sensing applications

Vijender Chahal
Department of Physics, Government College, Narnaul - 123001, Haryana, India
*Corresponding author, E-mail: vijenderchahal2@gmail.com

****Selection and Peer-Review under responsibility of the Scientific Committee of the National Conference on Advanced Engineering Materials (NCAEM 2022).**

ARTICLE HISTORY
Received: 12 Aug. 2022
Revised: 16 Nov. 2022
Accepted: 18 Nov. 2022
Published online: 27 Dec. 2022

KEYWORDS
Microring resonators; sensing; integrated optics.

ABSTRACT
To our knowledge, this is the first time that an analytical method for assessing integrated-optic microring resonators' sensing properties for use in chemical and biological sensing applications has been presented. This method uses an Airy functions analysis to take into account the polarised modes of the bent ring waveguide. The resonant frequencies thus obtained are shown to match reported numerical results quite well in the scalar domain. The study demonstrates that the sensitivity for both TE and TM polarisations grows with the detected medium's refractive index, but TE polarization's sensitivity is always greater than TM, which is contrary to what a straight waveguide approximation predicts.

1. Introduction

As channel add/drop filters and highly sensitive sensors for chemical and biological applications, integrated-optic microring resonators are increasingly being used in fiber-optic communication systems [1–5]. The top layer or cover layer of typical microring resonators, which are constructed as ridge or channel waveguides, acts as the sensing zone. Such devices' sensitivity is affected by the cover index as well as waveguide design factors such channel width, ring radius, core refractive index, and substrate refractive index. In addition, the usage of TE or TM polarised light affects the sensitivity. Accurate determination of the modal and polarisation parameters of wave propagation in the ring waveguide is required in order to assess the performance of such microring resonators. For this goal, a number of numerical approaches [1, 4, 5] as well as an analytical method [2] that operates in the scalar domain have been documented in the literature. An analytical approach to modelling the polarisation properties of ring waveguides has been put forth by Chao and Guo [3], but because it approximates the fields in curved waveguides with those of straight waveguides, it may not produce accurate results for microring resonators with very small radii (a few μm). Thus, it is necessary to determine the polarisation properties of such resonators while accounting for precise field patterns matching to curved waveguides.

Based on the Airy functions analysis of bent planar waveguides provided by Goyal et al. [6], we introduce for the first time in this study an analytical approach for figuring out the sensitivity of such microring resonators by taking the polarised modes of bent waveguides. By meeting the corresponding boundary conditions for the TE and TM polarisations of the real microring, polarisation dependencies are taken into account in the analysis. By comparing the method's findings to previously reported finite-difference time domain (FDTD) calculations, which are proven to closely match, the method is first validated in the scalar domain [1]. Thus, it is possible to determine the resonant frequencies and sensitivity in the C-band for the microring resonator taken into account in Ref. [3] as a function of the cover's refractive index and polarisation state.

Our calculations demonstrate both TE and TM polarisations are sensitive to changes in the detected medium's refractive index, but TE polarisation is always more sensitive than TM, which is contrary to what the straight waveguide approximation predicts. Furthermore, compared to the analysis in Ref. [3], the current technique yields much higher sensitivity values.

2. Theoretical model

We consider a type I waveguide-based microring resonator design as stated in Ref. [1], which is displayed in Figure 1, to describe and validate the method. With the use of low refractive index contrast GaAs/AlGaAs layers and side wall etching, this waveguide offers poor vertical confinement and significant lateral confinement at the GaAs/air contact. Using the effective index approach, the 3-D structure is converted to a comparable 2-D planar waveguide microring resonator, as shown in Figure 2.

Let its core thickness and radius of curvature be $2a$ and its cladding and core indices, n_1 and n_2, respectively. The scalar wave equation describing wave propagation inside the ring waveguide for $\rho >> a$ is given by [6]

$$\frac{d^2U}{dx^2}+k_0^2[N_e^2(x)-n_e^2]U(x)=0\,, \tag{1}$$

where n_e is the effective index, k_0 is the free space wave vector, and $(\rho+x)^{-1/2}U(x)=\psi(x)$ represents the modal field in the ring,. $N_e(x)$ is the equivalent refractive index profile of the bent waveguide given by

$$N_e^2(x)=n^2(x)+\Delta n^2(x).N(x)\,.$$

$N(x)$ describes the straight waveguide's refractive index profile and $\Delta n^2(x)$ is a tiny bending-induced disturbance and is given by

$$\Delta n^2(x)=\frac{1}{4R^2}+\frac{2}{\rho}\left(n_e^2-\frac{1}{4R^2}\right)x\,, \tag{2}$$

where $R=\rho k_0$. In this situation, the answers to Equation (1) can be expressed as [6]:

$$U(Z_1)=C_1Ai(Z_1)+D_1Bi(Z_1) \tag{3a}$$

$$U(Z_2)=C_2Ai(Z_2)+D_2Bi(Z_2) \tag{3b}$$

$$U(Z_3)=Ai(Z_3) \tag{3c}$$

where the subscripts on Z represent the three distinct zones as seen in Figure 2, and Zi is given by

$$Z_1=Z_3=\frac{\frac{RS^3}{2}-n_2^2-XS^3}{S^2} \tag{4a}$$

$$Z_2=\frac{\frac{RS^3}{2}-n_1^2-XS^3}{S^2} \tag{4b}$$

$$S^3=\frac{2}{R}\left(n_e^2-\frac{1}{4R^2}\right) \tag{4c}$$

where $X=xk_0$. By meeting the continuity requirements of U and dU/dx at the core-cladding boundaries, the constants C_i and D_i for scalar modes are derived and are given by

$$C_2=\pi[Ai(\delta)Bi^l(\gamma)-Ai^l(\delta)Bi(\gamma)] \tag{5a}$$

$$D_2=\pi[Ai(\delta)Ai(\gamma)-Ai^l(\delta)Ai(\gamma)] \tag{5b}$$

$$C_1=\pi[C_2Ai(\beta)+D_2Bi^l(\beta)Bi^l(\alpha) -(C_2Ai^l(\beta)+D_2Bi^l(\beta)Bi(\alpha)] \tag{5c}$$

$$D_1=\pi[C_2Ai(\beta)+D_2Bi^l(\beta)Ai(\alpha) -(C_2Ai(\beta)+D_2Bi(\beta)Ai^l(\alpha)] \tag{5d}$$

Each of the Airy functions' arguments is provided by

$$\alpha=\left(\frac{R}{2}-ak_0\right)S-\frac{n_2^2}{S^2} \tag{6a}$$

$$\beta=\left(\frac{R}{2}-ak_0\right)S-\frac{n_1^2}{S^2} \tag{6b}$$

$$\gamma=\left(\frac{R}{2}+ak_0\right)S-\frac{n_1^2}{S^2} \tag{6c}$$

$$\delta=\left(\frac{R}{2}+ak_0\right)S-\frac{n_2^2}{S^2} \tag{6d}$$

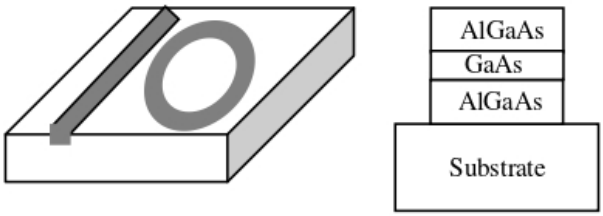

Figure 1: The type I ring resonator.

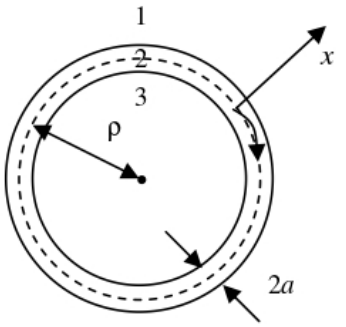

Figure 2: The equivalent 2-D bent planar waveguide.

Plotting $(C_2^2+D_2^2)/(C_1^2+D_1^2)$ as a function of ne yields Lorentzian peaks at various effective indices of the modes, and the breadth of the peak yields the imaginary portion of the effective index. This method yields the propagation constants. The round trip phase accumulated by the modal field must be an integral multiple of 2π in order to satisfy the resonance condition. Hence, the resonance wavelengths are as follows:

$$\lambda_m=\frac{2\pi\rho n_e}{m}\,, \tag{7}$$

where m is an integer denoting the resonance order. This formula yields the ring's equivalent leakage loss factor:

$$\alpha_L=\exp\left(-\frac{4\pi^2\rho n_{ei}}{\lambda_m}\right), \tag{8}$$

where n_{ei} is the imaginary component of the ring's effective propagation index. The 2-D structure with the following parameters is analysed using this: n_1 = 3.2, n_2 = 1.0, ρ = 4.85 μm, and $2a$ = 0.30 μm. The results for λ_m, free spectral range (FSR), and α_L for various resonance numbers m are displayed in Table 1. We should point out that Chin and Ho [2] employed a comparable methodology to determine the resonant wavelengths as well, but they used the effective ring radius in relation to the shifted peak of the fundamental mode. This approximation, in our opinion, is incorrect since the distance ξ along the axis of the ring waveguide is used to derive Eq. (1), which takes into account the phase factor $\exp(ik_0 n_e \xi)$ of the modes of the bent waveguide. This indicates that one should use the distance travelled along the axis rather than off-axis when determining the phase of the propagating mode and, consequently, resonance conditions. Table 1 also includes the values for λ_m and FSR from References 1 and 2, which were calculated using an FDTD technique. As is evident, compared to Ref. [2], our results match the FDTD ones more closely and also anticipate the ring's loss factor, whereas the other methods do not.

Table 1: Comparison of resonant wavelengths and FSR for the ring resonator

m	Ref. [2]		Present method			FDTD	
	λ_m (nm)	FSR (nm)	λ_m (nm)	FSR (nm)	Loss factor	λ_m (nm)	FSR (nm)
25	1611.22		1613.22		0.99951	1612.13	
		48.24		50.84			49.55
26	1562.29		1536.12		0.99986	1526.55	
		48.69		48.58			46.65
27	1520.28		1514.94		0.99908	1541.77	
		43.32		43.89			43.37
28	1480.26		1469.15		0.99998	1468.51	
		40.27		43.73			41.71
29	1429.30		1482.31		0.99929	1472.89	

We remark that the TE and TM polarised modes of the microring correspond to the TM-like and TE-like modes of the analogous planar curved waveguide, respectively, once the approach has been validated in the scalar domain. By meeting the continuity requirements of U and dU/dx for the TM mode and n^2U and dU/dx for the TE mode, the coefficients of Eq. (3) would then be achieved. The resulting adjusted expressions for C_i and D_i are as follows:

$$C_2 = \pi[F.Ai(\delta)Bi^{l}(\gamma) - Ai^{l}(\delta)Bi(\gamma)] \tag{9a}$$

$$D_2 = \pi[Ai^{l}(\delta)Ai(\gamma) - F.Ai^{l}(\gamma)Ai(\delta)] \tag{9b}$$

$$C_1 = \pi[C_2 Ai(\beta) + D_2 Bi^{l}(\beta)Bi^{l}(\alpha)/F - (C_2 Ai^{l}(\beta) + D_2 Bi^{l}(\beta)Bi(\alpha)] \tag{9c}$$

$$D_1 = \pi[C_2 Ai(\beta) + D_2 Bi^{l}(\beta)Ai(\alpha) - (C_2 Ai(\beta) + D_2 Bi(\beta)Ai^{l}(\alpha)/F] \tag{9d}$$

where n_1 is the effective index of TE (or TM) modes of the y-waveguide and the factor $F = n_2^2/n_1^2$ (or 1) for TE (or TM) polarizations of the microring,.

3. Evaluation of sensitivity

The sensitivity is given as follows for a microring resonator using resonant wavelength shift (RWS) sensing:

$$S_{RWS} = \frac{\partial \lambda_m}{\partial n_c}, \tag{10}$$

where n_c is the material's cover refractive index. This expression is broken down into device-related and waveguide-related sensitivities, which are assumed to be independent of one another, in the analysis provided by Chao and Guo [3].

$$S_{RWS} = \frac{\partial \lambda_m}{\partial n_c} = \frac{\partial \lambda_m}{\partial n_e}.\frac{\partial n_e}{\partial n_c} = S^{D}_{RWS}.S^{W}_{RWS}. \tag{11}$$

The device sensitivity S^{D}_{RWS} used in their analysis is equal to $2\pi\rho/m$ and is derived from the resonance condition (Eq. (7)). By roughly comparing the fields in a straight waveguide to those in the ring, the waveguide sensitivity S^{W}_{RWS} is obtained. In our approach, we use the modified expressions of Eq. (9) in the previous study to directly determine the total sensitivity S_{RWS} by monitoring the variation in λ_m owing to n_c for both TE and TM modes.

We adopt the identical microring resonator configuration as in Ref. [3], which consists of a polystyrene ridge with dimensions of 1.8 μm in thickness and 1.5 μm in width resting on a substrate made of SiO_2 and Si, to compare our findings with the analysis mentioned above. The ring's radius is assumed to be 30 μm, and the refractive indices of polystyrene, silicon dioxide, and silicon are assumed to be 1.57, 1.444, and 3.42, respectively, at 1550 nm. With a refractive index range of 1.0 (air) to 1.57, the cover acts as the sensor area (polystyrene). In order to keep things practical, we only take into account resonance orders that are in the C-band (λ_m = 1525-1575 nm).

Figure 3 displays for the TE (solid) and TM (dashed) polarizations, λ_m as a function of n_c with m ranging from 178 to 186. The two polarisations differ noticeably, as can be seen plainly, suggesting a strong polarisation dependence. Figure 4 displays the RWS sensitivity for TE (solid) and TM (dashed) polarisations, as determined by Eq. (10). The upper curves in

each group correspond to a lower m value. It can be seen that TE modes exhibit more sensitivity than TM modes, and that sensitivity rises with n_c. This rise can be due to the fact that when n_c increases, the modal field spreads further into the cover, increasing its propensity to interact with the medium being sensed.

The curves from Figure 4 for m = 182 are shown in Figure 5, along with the comparable curves that were produced using the straight waveguide assumption from Ref. [3]. This graph demonstrates that the current strategy greatly outperforms Ref. [3] in terms of sensitivity value. This is to be expected since the bent waveguide fields interact more with the detected medium and spread into the cover region than the straight waveguide. This results in greater sensitivity. Another intriguing finding is that, contrary to what the straight waveguide approximation of Ref. [3] suggests, the present analysis predicts higher sensitivity for TE polarisations than TM for all values of n_c.

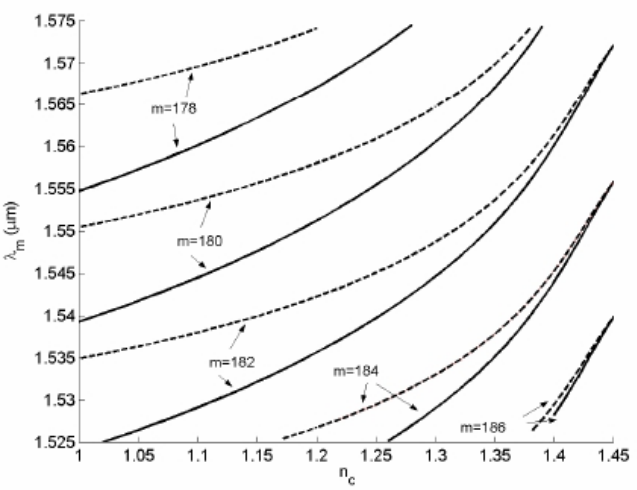

Figure 3: λ_m versus n_c for TE (solid) and TM (dashed).

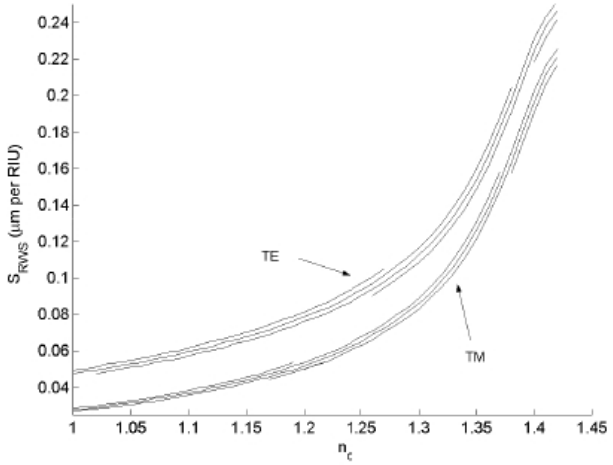

Figure 4: *SRWS* versus n_c for various values of m.

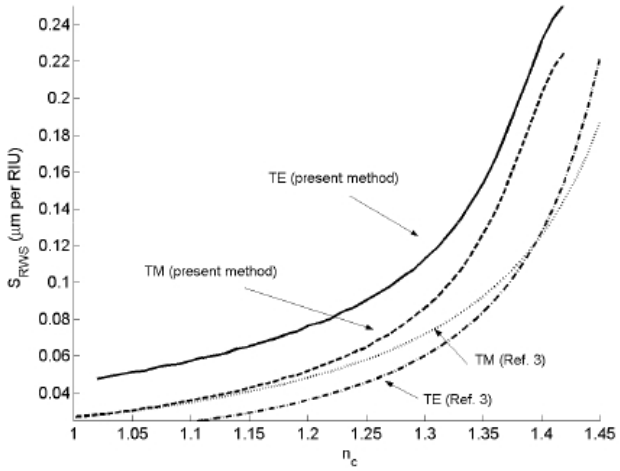

Figure 5: *SRWS* versus n_c using present method and the analysis of Ref. [3] (m = 182).

4. Conclusions

By adding polarisation dependencies of the fields of bent waveguides, we have presented an analytical method for analysing the sensing properties of microring resonators for chemical and biological applications in terms of resonant wavelength changes. The findings show that there is a considerable polarisation dependence on resonant wavelengths and sensitivities, and that for both TE and TM polarisations, sensitivity increases with increasing refractive index of the detected medium. Moreover, the straight waveguide approximation incorrectly predicts that the TE polarisation is more sensitive than the TM for the given waveguide characteristics.

References

[1] S.C. Hagness, D. Rafizadeh, S.T. Ho, A. Taflove, FDTD microcavity simulations: design and experimental realization of waveguide-coupled single-mode ring and whispering-gallery-mode disk resonators, *IEEE J. Lightwave Technol.* **15**(1997) 2154 -2165.

[2] M.K. Chin; C. Youtsey; W. Zhao; T. Pierson; Z. Ren; S.L. Wu; L. Wang; Y.G. Zhao; S.T. Ho, GaAs microcavity channel-dropping filter based on a race-track resonator, *IEEE Photon. Technol. Lett*. **11** (1999) 1620-1622.

[3] J.K.S. Poon, L. Zhu, G.A. DeRose, A. Yariv, Transmission and group delay of microring coupled-resonator optical waveguides, *Opt. Lett*. **31** (2006) 456-458.

[4] J.E. Heebner, R.W. Boyd, Enhanced all-optical switching by use of a nonlinear fiber ring resonator, *Opt. Lett*. **24** (1999) 847–849.

[5] M.K. Chin, Polarization dependence in waveguide-coupled micro-resonators *Opt. Exp.* **11** (2003) 1724-1726 .

[6] I.C. Goyal, R.L. Gallawa, A.K. Ghatak, Bent planar waveguides and whispering gallery modes: A new method of analysis, *IEEE J. Lightwave Technol.* **8** (1990) 768-774.